

Pelvic B1 mapping at 3T for DCE

R. D. Newbould¹, and B. Whitcher¹

¹GSK Clinical Imaging Centre, London, United Kingdom

Introduction: Ovarian cancer is the fourth most common cause of cancer mortality in women. Much work has therefore been done to develop early assessments of tumour response, such as dynamic contrast enhanced (DCE) perfusion measurements [1]. In order to better quantify contrast agent concentration, it is common to use T1 maps rather than relative changes in signal intensity from T1-weighted images [2] before and during contrast agent administration. In order to acquire T1 maps with sufficient temporal resolution for DCE, most work relies on the variable-flip-angle method (VFA), where multiple spoiled gradient echoes (SPGR) are taken at different flip angles [3]. However, its application in the body at 3T is hampered by the pronounced variation in the B1-field, introducing large errors in the estimated T1 values [4].

Materials and Methods: Dynamic T1 maps were acquired before and during a sham DCE examination performed on a phantom and on a healthy female volunteer with a Siemens 3T Verio scanner. The VFA SPGR sequences acquired 16 5-mm slices in a 3D slab located in the pelvis, (TR=4.22ms TE=1.23ms FOV=250mm, 5mm slc, 25% phase and 25% slab oversampling, TA=5s, phase encoding=L/R). Due to their rapid acquisition time, 11 flip angles were taken from 2° to 25° with 5 averages before the dynamic series. The dynamic series used a single average and a flip angle of 16°. T1 values were estimated via direct nonlinear fitting to the SPGR signal equation (Eq 1):

$$S(\alpha) = PD \frac{\sin(\alpha) \cdot (1 - \exp(-TR/T_1))}{(1 - \cos(\alpha) \cdot \exp(-TR/T_1))} \cdot \exp(-TE/T_2^*) \quad [1]$$

$$S(B_1\alpha) = PD \frac{\sin(B_1\alpha) \cdot (1 - \exp(-TR/T_1))}{(1 - \cos(B_1\alpha) \cdot \exp(-TR/T_1))} \cdot \exp(-TE/T_2^*) \quad [2]$$

B1 maps were acquired using Cunningham's saturated double-angle method (SDAM) [5]. The SDAM acquisition took 16 2D-EPI slices in identical locations as the VFA method using a 64x64 matrix. A 1.5-ms composite 90°_x pulse [6] saturated spins, and was followed by 500ms of saturation recovery time before all slice readouts in a total TR of 1.5s. The sequence alternated between 60° and 120° excitation pulses for 10 volumes in 15 seconds. B1 maps were estimated via $B_1(x,y) = \cos^{-1}(I_{120}/(2 \cdot I_{60}))$, and B1-corrected T1 fits were performed using Eq 2.

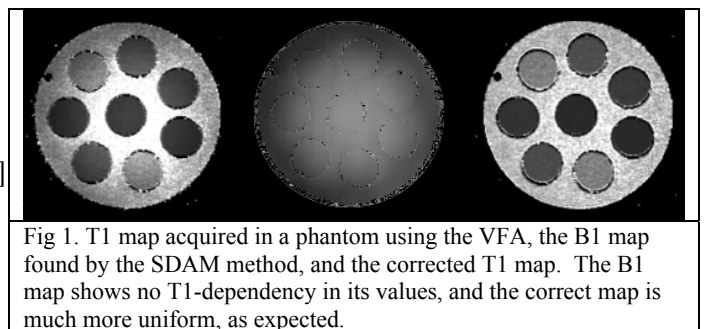


Fig 1. T1 map acquired in a phantom using the VFA, the B1 map found by the SDAM method, and the corrected T1 map. The B1 map shows no T1-dependency in its values, and the correct map is much more uniform, as expected.

Results: Fig 1 shows the variation in the VFA-determined T1 map. The phantom consists of vials of various T1s inside a larger uniform cylinder. The B1 map (centre) shows the increased flip angle in the centre of the phantom, which results in a more uniform T1 after correction (right). Figs 2 and 3 show the same process applied in the pelvis (colorbars range from 0 to 1200-ms). Four of the 16 slices are shown for brevity. The muscles in the pelvis show a marked increase in the T1 estimate laterally before the correction; this non-uniformity is helped by the correction.

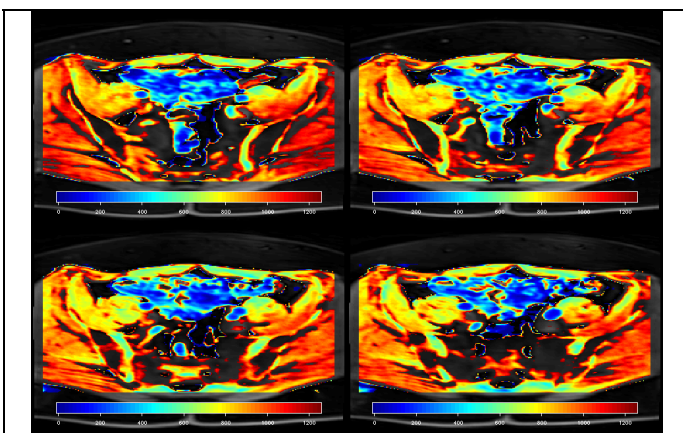


Fig 2. T1 maps through the pelvis acquired using the VFA technique. Increased T1 values are observed peripherally.

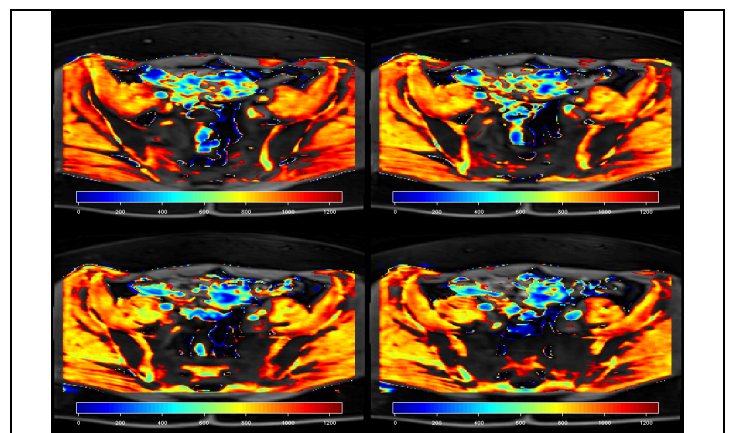


Fig 3. B1-corrected T1 maps in identical locations as Fig 2. Note flatter profile throughout the muscle.

Discussion: The double angle method requires a long TR to ensure no T1 weighting remains in the acquired images. This is prohibitive in the abdomen, where the presence of fluid would require 15+ seconds for each image of each slice. Using the SDAM method, we acquired ten volumes of 16-slice B1 maps in 15 seconds. Ten volumes were specifically chosen to accommodate a modest breath-hold. Fewer volumes and increased coverage may be used instead. The B1-corrected dynamic series has now been integrated into a body DCE study at 3T; i.e. evaluating therapies in primary and secondary ovarian masses.

References: 1. Hayes, *NMR Biomed.* 2002;**15**:154–163. 2. Rosen, *MRM*; **14**:249-265, 1990. 3. Fram, *MRI*; **5**:201-208, 1987. 4. Venkatesan, *MRM*; **40**:592-602, 1998. 5. Cunningham, *MRM*; **55**:1326-1333, 2006. 6. Levitt, *Progress in NMR Spectroscopy*; **18**:61-122, 1986.